(4)

THERMOMECHANICAL CONTACT PHENOMENA AND WEAR OF SLIDING SEAL COMPONENTS

Annual Report 1987

submitted to

Office of Naval Research

Contract No. N00014-87-K-0125
Period Covered:
January 1, 1987 to December 31, 1987

by

Francis E. Kennedy, Jr.
Professor of Engineering

and

Beda M.M. Espinoza and Susanne M. Pepper
Graduate Research Assistants

Thayer School of Engineering
Dartmouth College
Hanover, New Hampshire 03755

March 1988

Unclassified
SECURITY CLASSIFICATION OF THIS PAGE

REPORT DOCUMENTATION PAGE

1a. REPORT SECURITY CLASSIFICATION Unclassified	1b. RESTRICTIVE MARKINGS
2a. SECURITY CLASSIFICATION AUTHORITY	3. DISTRIBUTION / AVAILABILITY OF REPORT Approved for public release; distribution unlimited
2b. DECLASSIFICATION / DOWNGRADING SCHEDULE	
4. PERFORMING ORGANIZATION REPORT NUMBER(S) Annual Report 1987	5. MONITORING ORGANIZATION REPORT NUMBER(S)
6a. NAME OF PERFORMING ORGANIZATION Dartmouth College 6b. OFFICE SYMBOL (*If applicable*)	7a. NAME OF MONITORING ORGANIZATION Office of Naval Research
6c. ADDRESS (*City, State, and ZIP Code*) Thayer School of Engineering Hanover, NH 03755	7b. ADDRESS (*City, State, and ZIP Code*) Engineering Science Directorate Arlington, Virginia 22217
8a. NAME OF FUNDING / SPONSORING ORGANIZATION Office of Naval Research 8b. OFFICE SYMBOL (*If applicable*)	9. PROCUREMENT INSTRUMENT IDENTIFICATION NUMBER N00014-87-K-0125
8c. ADDRESS (*City, State, and ZIP Code*) Engineering Science Directorate Arlington, Virginia 22217	10. SOURCE OF FUNDING NUMBERS PROGRAM ELEMENT NO. 61153N 24 / PROJECT NO. NR 091-044 / TASK NO. RR024-03-03 RMS2403-032 / WORK UNIT ACCESSION NO. 4316004
11. TITLE (*Include Security Classification*) Thermomechanical Phenomena and Wear of Sliding Seal Components	
12. PERSONAL AUTHOR(S) Francis E. Kennedy, Jr., Beda M.M. Espinoza and Suzanne M. Pepper	
13a. TYPE OF REPORT 13b. TIME COVERED FROM 87/1/1 TO 87/12/31	14. DATE OF REPORT (*Year, Month, Day*) 1988 March 30 15. PAGE COUNT
16. SUPPLEMENTARY NOTATION	

17. COSATI CODES		
FIELD	GROUP	SUB-GROUP
11	01	

18. SUBJECT TERMS (*Continue on reverse if necessary and identify by block number*)
Mechanical Face Seals, Wear, Friction, Ceramic Coatings, Thermal Stress.

19. ABSTRACT (*Continue on reverse if necessary and identify by block number*)

The objectives of this investigation were to better understand the tribological behavior of ceramic-coated rings sliding against carbon graphite and the thermocracking that occurs with some of the ceramic coatings. Sliding wear tests were conducted on Inconel 625 substrates coated with four different hard materials: chromium oxide, chromium carbide, titanium nitride, and tungsten carbide. Tests were also run to determine the corrosion behavior of the ceramic-coated rings in seawater. Surface profilometry, mass loss measurements, and microscopy were used to characterize wear, cracking and corrosion phenomena. Coupled with the experimental work was a theoretical analysis of temperatures and stresses in the contact region of the ceramic coating during sliding. The influence of various material and geometric parameters on coating cracking was studied in the analytical work.

20. DISTRIBUTION / AVAILABILITY OF ABSTRACT ☒ UNCLASSIFIED/UNLIMITED ☐ SAME AS RPT ☐ DTIC USERS	21. ABSTRACT SECURITY CLASSIFICATION
22a. NAME OF RESPONSIBLE INDIVIDUAL M.B. Peterson	22b. TELEPHONE (*Include Area Code*) 22c. OFFICE SYMBOL

DD FORM 1473, 84 MAR 83 APR edition may be used until exhausted. All other editions are obsolete.

SECURITY CLASSIFICATION OF THIS PAGE

THERMOMECHANICAL CONTACT PHENOMENA AND WEAR OF SLIDING SEAL COMPONENTS

Annual Report 1987

submitted to

Office of Naval Research

Contract No N00014-87-K-0125
Period Covered: January 1, 1987 to December 31, 1987

by

Francis E. Kennedy, Jr.
Professor of Engineering

and

Beda M.M. Espinoza and Susanne M. Pepper
Graduate Research Assistants

Thayer School of Engineering
Dartmouth College
Hanover, New Hampshire 03755

March 1988

FOREWORD

Work at the Thayer School of Engineering at Dartmouth College on this research project has been sponsored by Office of Naval Research Contract Number N00014-87-K-0125. Drs. Peter J. Blau and A.William Ruff have been the ONR Scientific Officers for the project during the past year.

The authors gratefully acknowledge the assistance of V.A. Surprenant in metallographic work and the personnel of the Dartmouth Electron Microscope Facility, particularly Ms. Louisa Howard, for assistance with scanning electron microscopy. Union Carbide Corp. and EG & G Sealol contributed materials for use in the test program. Drs. J.A. Sue and R.C. Tucker of Union Carbide Corp. offered beneficial advice during the past year. The authors are grateful for that assistance.

ABSTRACT

The objectives of this investigation were to better understand the tribological behavior of ceramic-coated rings sliding against carbon graphite and the thermocracking that occurs with some of the ceramic coatings. Sliding wear tests were conducted on Inconel 625 substrates coated with four different hard materials: chromium oxide, chromium carbide, titanium nitride, and tungsten carbide. Tests were also run to determine the corrosion behavior of the ceramic-coated rings in seawater. Surface profilometry, mass loss measurements, and microscopy were used to characterize wear, cracking and corrosion phenomena. Coupled with the experimental work was a theoretical analysis of temperatures and stresses in the contact region of the ceramic coating during sliding. The influence of various material and geometric parameters on coating cracking was studied in the analytical work.

TABLE OF CONTENTS

LIST OF FIGURES

LIST OF TABLES

1.0 INTRODUCTION

Like many other sliding components, the seal rings of mechanical face seals must be able to withstand many hours of continuous sliding contact during operation. The wear that occurs during that contact frequently determines the useful life of a seal ring. Seal designers have attempted to increase seal durability by choosing hard, wear-resistant seal ring materials. Ceramic materials, such as silicon carbide, have proven to be good candidates for many severe seal conditions because of their high hardness and good wear resistance [1]. Most ceramics are somewhat difficult to form in the shapes and sizes required for large face seals, however, and their brittleness necessitates great care in handling and mounting. There is interest in achieving the wear resistance of ceramics without the production and handling difficulties associated with monolithic ceramics. One way to do so is to apply a thin coating of ceramic to a readily-formed, ductile metallic substrate. Ceramic-coated seal rings have met with success in many applications, but their use in salt water seals has been limited. Problems that could lead to foreshortened lives of ceramic-coated seal rings include spalling [3] and thermo-cracking [4] of the ceramic coatings. Another problem has been corrosion in the salt water environment, particularly crevice corrosion at the coating/substrate interface [2].

Despite these potential problems, ceramic coatings are of interest in mechanical face seals because they have been shown to have nearly as good wear resistance as monolithic ceramics in sliding tests [3]. The coatings in that study were on substrates of either iron- or copper-based materials. Tribe [2] showed, however, that ceramic coatings on those substrates can experience pitting or crevice corrosion in salt water. There was little evidence of corrosion, though, for the same coatings on a corrosion-resistant substrate of Inconel 625 [2]. That nickel-based alloy is now being used successfully in many marine components requiring good resistance to corrosion in seawater, including some components of face seals. For that reason, this project concentrated on the study of several promising ceramic coatings on Inconel 625 substrates. Of particular interest

were the tribological performance of the coatings in sliding contact against carbon graphite seal rings, the failure mechanisms that could limit the usefulness of the coatings, and the corrosion resistance of the coating/substrate system.

Four different coatings were studied. They included chromium oxide, chromium carbide, titanium nitride and tungsten carbide. These four coating materials are among the most effective hard coatings developed in recent years and are used for a variety of tribological applications [5]. Several boride coatings were also tested, but they proved to wear excessively in initial tests and were not tested completely. The goal of the project was an improved understanding of the factors influencing wear, thermocracking and other mechanisms of coating failure mechanisms. To achieve this goal, the project consisted of both experimental and numerical activities.

2.0 EXPERIMENTAL

2.1 Tribotest Methods

The tribotests were carried out on a test machine previously used for both wear studies and face seal research [6]. The machine is a converted drill press, with each of two test spindles being driven by a separate motor. The spindles were gear driven at a preset speed of 1800 rpm for this work. In most tests a normal load of either 50N or 100N was applied through the spindles by static weights hung on the loading arm. A ceramic-coated seal ring was mounted at the end of the rotating spindle. Beneath each spindle was a specimen-holding platform mounted on a thrust bearing. A stationary seal ring was mounted in that specimen holder. Rotation of the specimen holder was limited by a torque-sensing system for continuous measurement of friction.

The stationary specimen was a commercial seal ring made of carbon graphite. It had a mean diameter of 5 cm and a face width of 2.5 mm, and those dimensions dictated the nominal contact area between the seal faces. The rotating ceramic-coated ring had a slightly greater face width and was mounted concentric with the stationary ring. With these ring dimensions, the sliding velocity at the contact interface was 4.7 m/s and the nominal contact pressure was 0.25 MPa for the 100N load cases and 0.125 MPa with 50N load.

Prior to testing, the contacting faces of most rings were hand lapped and polished, with alumina grit being used for the carbon graphite ring and diamond lapping/polishing compound for the hard coatings. Some of the coated rings (those coated with TiN) were not re-lapped because of the coating thinness. The surface topography of each ring was characterized using a computer-assisted profilometry system. The test specimens were ultrasonically cleaned and weighed on an accurate analytical balance both before and after each test.

All tests were run dry (no sealed fluid) and at room temperature. The tests were not meant to simulate the performance of an ideal seal, which would have a thin layer of sealed fluid between the flat seal faces. In actual seals it is known that there is some contact between the solid seal faces and this solid/solid contact is responsible for wear of

the seal rings [6]. These tests were meant to determine the tribological behavior of the seal rings when subjected to solid/solid contact.

Most tests were run for either 6 or 12 hours, giving a total sliding distance of 100 km or 200 km, respectively. For each material there were at least 6 tests of either 6 or 12 hour duration, along with one test lasting 30 hours for a sliding distance of 500 km. The friction force was monitored continuously during each test. At the conclusion of a test the seal was disassembled and each ring was ultrasonically cleaned and dried before being re-weighed on the analytical balance. The surface topography was again characterized and the ring surfaces were examined using optical and scanning electron microscopy.

2.2 Materials

The substrate for all of the coated rings tested in this study was Inconel 625, a nickel-based alloy with proven corrosion resistance. Tribe's work on ceramic coatings exposed to a seawater environment had previously shown that this substrate material was very resistant to corrosive attack in salt water, unlike steel substrates [2]. The major components of the material are nickel (61%), chromium (21.5%) and molybdenum (9%). The material was machined to a ring shape with 5.5 cm outside diameter, 4 cm inside diameter and 0.6-0.7 cm thickness. Prior to being coated the rings were degreased, ultrasonically cleaned, and sputter cleaned. The rings were then coated with one of four different hard coatings, tungsten carbide (WC), chromium oxide (Cr_2O_3), chromium carbide (a mixture of Cr_7C_3 and Cr_3C_2) , or titanium nitride (TiN).

The chromium oxide coating was applied by plasma spraying on a pre-roughened surface. No bond coat was used and micrographs of the interface (Figure 1) showed that mechanical interlocking was the predominant means of bonding between coating and substrate. Cross-sections, such as that shown in Figure 1, revealed that the coating thickness was 350 - 375 μm. The coated surfaces were lapped and polished to a surface roughness of about 0.1μm Ra.

FIGURE 1. Cross-section of plasma-sprayed chromium oxide coating on Inconel 625 substrate. (250X magnification)

FIGURE 2. Cross-section of chromium carbide coating H on Inconel 625 substrate. Coating was lapped after detonation gun spraying. (200X magnification)

Two slightly different chromium carbide coatings were tested. Both coatings had the same chemical composition, consisting of 80% chromium carbide (92 Cr - 8 C) and 20% nickel chromium (80 Ni - 20 Cr). The only difference between the two coatings was the size distribution of the nickel chromium particles, -44 μm for one coating, designated C, and -20 μm for the other, designated H. Both coatings were applied by the detonation gun thermal spray process and had an as-sprayed thickness of about 250 μm. The coatings were lapped and polished to a roughness of Ra ≤ 0.1 μm prior to the wear tests. A micrograph of a typical cross-section of a lapped coating is shown in Figure 2. A recent study of the same two chromium carbide coatings by Sue and Tucker [8] showed that the coating with the smaller nickel chromium particle size, coating H, had more resistance to erosion by solid particles over a large range of temperatures. They also found that coating C was slightly more dense and harder than coating H. There does not appear to have been a comparison of the sliding wear behavior of the two chromium carbide coatings prior to this investigation, at least not in a seal configuration.

The tungsten carbide coatings were also applied by a plasma spray process. The sprayed powder included a nickel and cobalt binder, in addition to WC. To further promote the formation of a metallurgical bond between coating and substrate, the coated rings were heat treated after spraying. During the heat treatment, diffusion between the 250 μm thick coating and the nickel- based substrate resulted in a diffusion layer as is shown in Figure 3. No distinct interface between coating and substrate could be noted, in contrast to the chrome oxide coatings. The coated surface was lapped and polished after heat treatment to a 0.1μm Ra roughness.

The titanium nitride coatings were applied by a physical vapor deposition (PVD) process (vacuum arc evaporation) at a coating temperature of slightly less than 500°C. The ring surfaces were lapped flat before being polished. The PVD process is rather slow and is normally used to produce very thin coatings [5]. Earlier tests [3] had shown that seal rings with thin (5 μm or less) TiN coatings did not have good long-term durability. For that reason, thicker TiN coatings were used in this study. First a thin bond coat of pure titanium

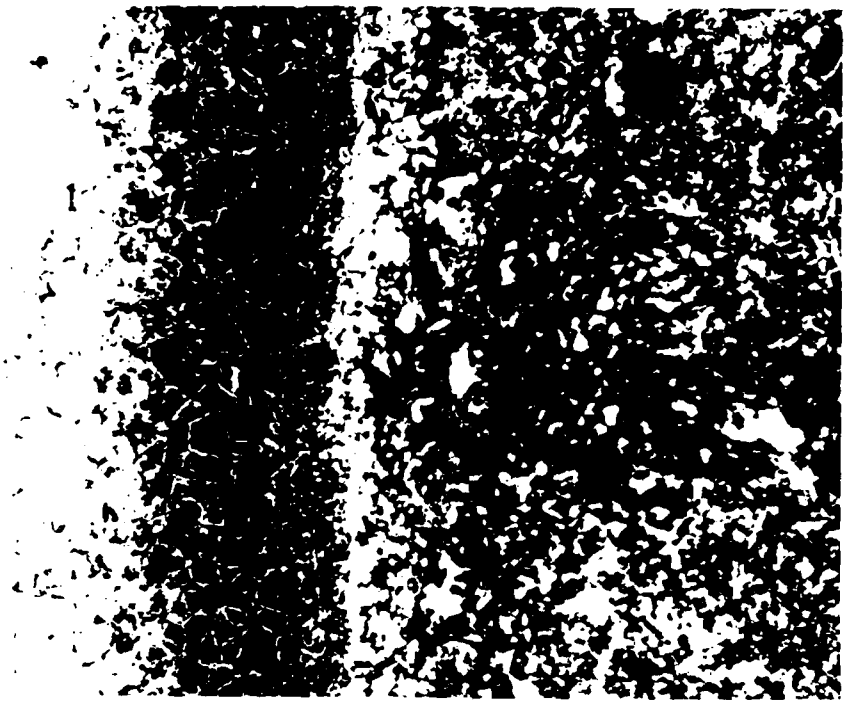

FIGURE 3. Cross-section of plasma-sprayed and heat treated tungsten carbide coating on Inconel 625 substrate. (250X magnification)

FIGURE 4. Cross-section of PVD-deposited titanium nitride coating on Inconel 625 substrate. (600X magnification)

was deposited on the lapped Inconel 625 surface, and this was followed by a 5μm thick layer of TiN. The coated surface was then sputter cleaned and another thin titanium bond coat was applied, followed by a 20μm thick titanium nitride layer. The resulting 25μm thick TiN coating is shown in cross-section in Figure 4.

In all tribotests, the coated rings were slid against a commercial seal ring made from a resin-impregnated grade of carbon graphite. The same grade of carbon graphite was used throughout the test program.

2.3 Corrosion Tests

For the corrosion tests, coated rings of each material were cut into sections of approximately 1 cm length. Both worn and unworn rings were sectioned. One cross-sectional face of each specimen was ground and polished and the specimens were then cleaned and accurately weighed. Each was placed in a salt water solution representative of seawater and the solution was agitated by means of a magnetic stirrer. The containers were sealed to prevent evaporation and were left at room temperature for 30 and 60 day periods. The specimens were then dried and re-weighed and viewed in optical and scanning electron microscopes to look for evidence of corrosion, particularly at the coating/substrate interface and on the friction surface.

2.4 Results of Tribotests

The four coating materials studied intensively in this series of tests all showed very low wear rates, comparable in magnitude to the wear rates measured earlier for similar coatings on different substrates and almost as low as the wear of silicon carbide measured in the earlier study [3]. A summary of the wear data is given in Tables 1 and 2. The first set of tests was run at 100 N normal load and the results of those tests are given in Table 1. The volumetric wear rate of WC proved to be slightly lower in those tests than the wear rate of Cr_2O_3 or TiN, although Cr_2O_3 had a lower wear rate than WC on a mass loss basis.

The remainder of the tests were run at a normal load of 50 N. Results of the 50 N tests are given in Table 2. Comparison of the data in Tables 1 and 2 shows that there was little influence of normal load on the wear rate of the tungsten carbide coating. The carbon graphite ring in contact with WC, however, showed a wear rate that was approximately proportional to load. From the 50 N tests it can be seen that the chromium carbide coatings exhibited the lowest wear rates of any of the coatings tested in this study.

The carbon graphite wear rate was generally about 50 times greater than the wear rates of the coatings, but in all cases it was less than had been measured in tests of reaction-sintered silicon carbide rings [3]. Slightly more carbon graphite wear occurred in the tungsten carbide tests than with the other three coating materials. Even after correcting for the effect of load on wear, the carbon graphite wear against the chromium carbide materials was less than against the other coating materials.

There was no major difference noted in the friction coefficient for the different coating materials. In all cases the friction coefficient was at or slightly below 0.10. As had been found in the earlier study, there were occasional bursts of higher friction. The buildup of third body wear debris appeared to be responsible for the friction bursts.

Each of the coating materials showed its own peculiarities and they will be discussed separately.

TABLE 1

RESULTS OF WEAR TESTS AT 100 N NORMAL LOAD

Wear data are given in terms of both mass lost / sliding distance (mg/km)
and linear wear / sliding distance (μm/km)
(Standard deviations shown in parentheses)

	Coating Wear		Carbon Graphite Wear	
Coating	mg/km	μm/km	mg/km	μm/km
Cr_2O_3	0.0069 (σ = 0.0023)	0.0031	0.43 (σ = 0.14)	0.54
TiN *	0.0091 (σ = 0.0076)	0.0039	0.34 (σ = 0.19)	0.43
**	0.93		17.1	
WC	0.0102 (σ = 0.0031)	0.0021	0.58 (σ = 0.27)	0.73

* data from tests of TiN coating in which no coating failure occurred
** data from test of TiN coating in which coating failure occurred

TABLE 2

RESULTS OF WEAR TESTS AT 50 N NORMAL LOAD

Wear data are given in terms of both mass lost / sliding distance (mg/km)
and linear wear / sliding distance (μm/km)
(Standard deviations shown in parentheses)

	Coating Wear		Carbon Graphite Wear	
Coating	mg/km	μm/km	mg/km	μm/km
Tungsten Carbide	0.010 (σ = 0.008)	0.0021	0.257 (σ = 0.13)	0.32
Chromium Carbide C	0.0039 (σ = 0.0014)	0.0012	0.173 (σ = 0.087)	0.22
Chromium Carbide H	0.0034 (σ = 0.0009)	0.0012	0.139 (σ = 0.12)	0.18

2.4.1 Tungsten Carbide

The wear process for the tungsten carbide coatings appeared to begin with wear of the metallic binder, causing the carbide particles to stand a bit proud of the surface. The carbides then wore slowly by a polishing process, resulting in flat carbide particles, as is seen in Figure 5. The result of this process was a decrease in the surface roughness of the carbide coating (from an average of about 0.15 μm Ra to about 0.10 μm Ra). The rings had been heat treated after coating, causing a metallurgical bond to form between coating and substrate. This is in contrast to the mechanical bond usually formed between plasma-sprayed coatings and substrate. This heat treatment did not seem to affect the wear of the coating, and the composition of the substrate also seemed to have little effect. The wear rates measured in this study were similar to those measured earlier for un-heat treated tungsten carbide coatings on different substrates [3].

As was mentioned above, a decrease in normal load by a factor of two had very little effect on the wear rate of the tungsten carbide coating, but decreased the carbon graphite wear by about a factor of two. Examination of the worn surfaces after tests at the two different loads showed no evidence of the influence of load on surface appearance or on apparent wear mechanisms.

There was no evidence of any debonding or cracking for the WC coatings in this study, although there was some microscopic pitting on the contact surface. The pits were fewer in number with the heat treated coating than in the earlier study. Some of the pits appeared to be originally pores in the coating, such as the small pit or pore shown on the surface in Figure 5. Other pits appeared to have been the result of fatigue, resulting in the removal of a carbide particle. An example is shown in Figure 6. The particles during the formation of a pit such as that in Figure 6 could have remained as third bodies between the sliding surfaces, contributing to the wear of the carbon graphite ring surface.

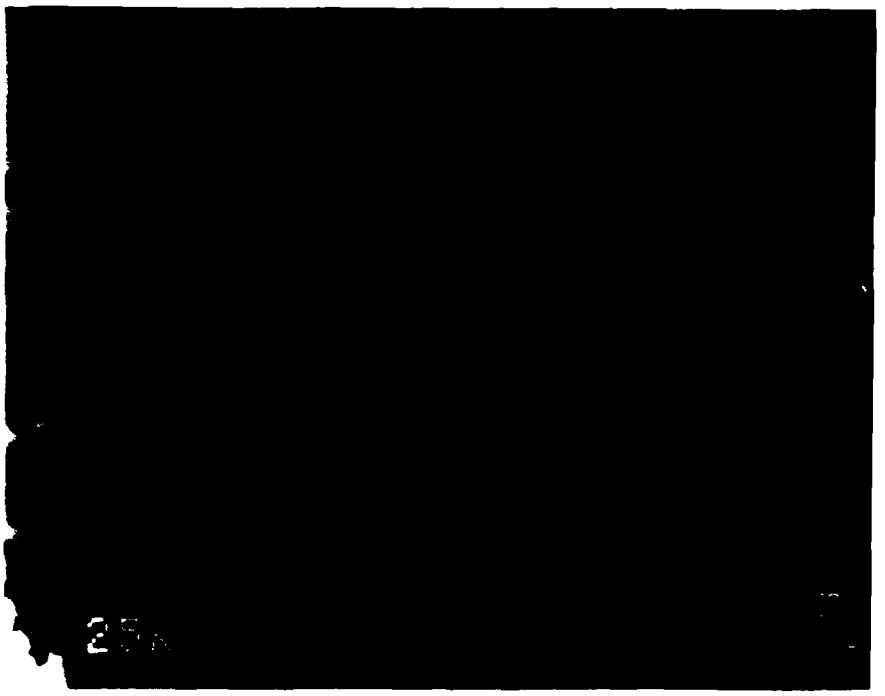

FIGURE 5. Worn surface of tungsten carbide coating. (5500X magnification)

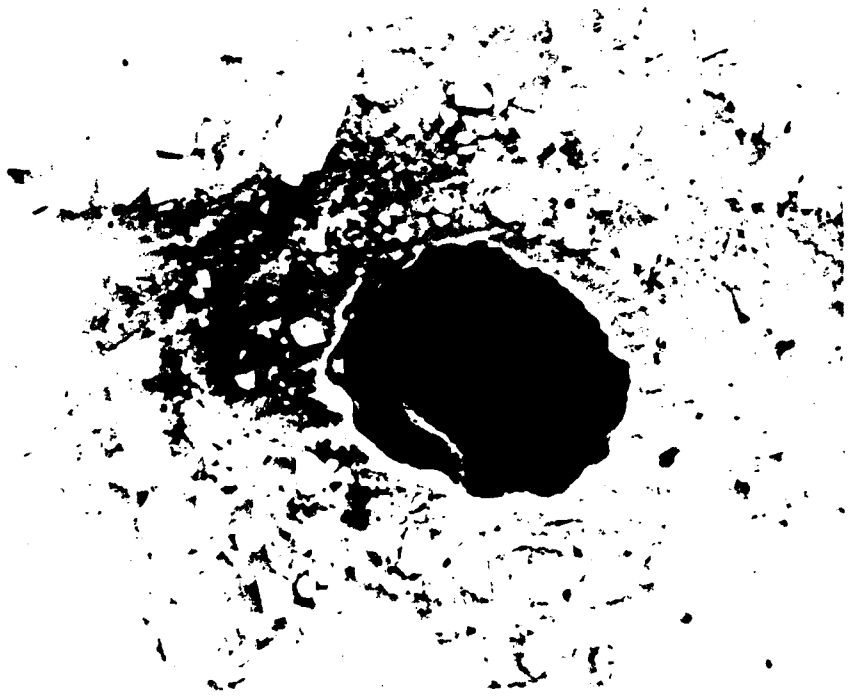

FIGURE 6. Worn surface of tungsten carbide coating showing pit. (1200X magnification)

2.4.2 Titanium Nitride

The TiN coatings were found to wear by polishing of the surface asperities (burnishing), resulting in a decrease in surface roughness during the first few hours of testing. There was some evidence of light abrasion of the carbon graphite surface by small third body particles (presumably TiN wear debris), but the wear was small until later stages of testing, when the TiN coating had worn very thin. Evidence of the decrease of coating thickness due to wear is shown in Figure 7. Wearthrough of the coating resulted in a sharp increase in wear of both ceramic-coated ring and carbon graphite surface. Data are given in Table 1 which show that the TiN wear rate increased by about two orders of magnitude when coating failure occurred, and the carbon graphite wear increased almost as much. The cause of the increased wear rates was the presence of hard TiN debris between the two sliding surfaces. There was evidence that spalling of the TiN coating had occurred when the coating became very thin. This spalling had also been noted in earlier tests of thinner TiN coatings on different substrates [3]. The wear rate for the thicker coatings used in this study was similar to that for thin TiN coatings, and therefore they lasted longer than the thin coatings, but they still suffered from significantly increased wear rates when wearthrough did occur.

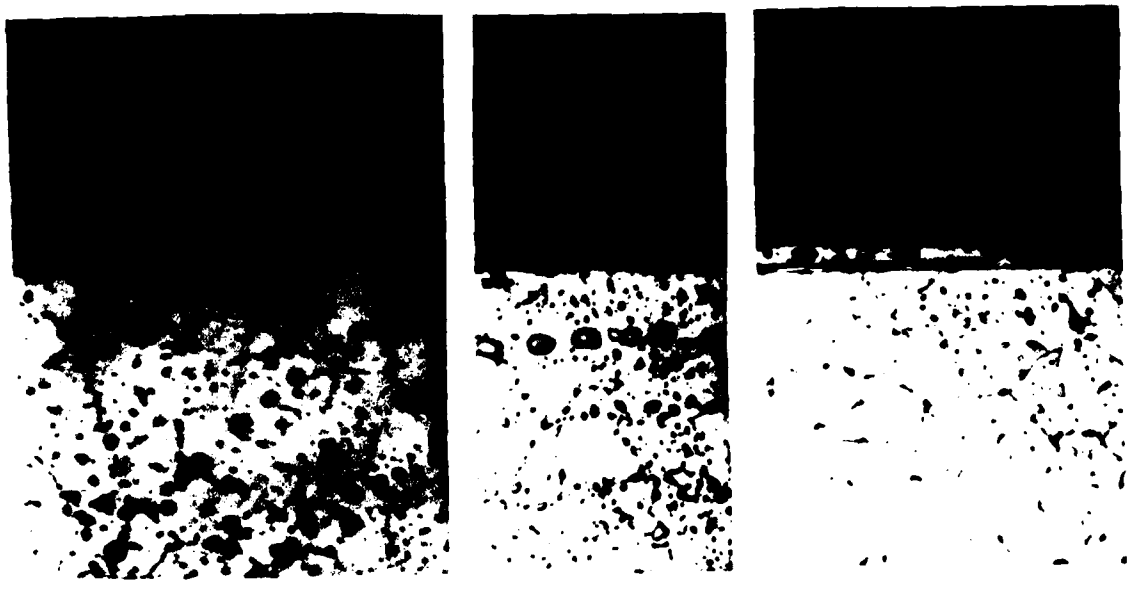

FIGURE 7. Cross-sections of titanium nitride coating outside wear track (left), at edge of wear track (center), and at center of wear track (right). (800X magnification)

With the titanium nitride coatings, as with all of the other coatings tested in this study, there was some transfer of carbon graphite to the coating surface. An example of this transfer is shown in Figure 8. The thin, discontinuous film of transferred carbon appeared to be adhered, albeit not strongly, to the coating surface, and its presence would serve to limit direct contact between the two ring surfaces. In addition to the transferred carbon, there were also loose particles of carbon graphite wear debris on the contact surfaces. These third body particles appeared to build up over time and were responsible for the bursts of higher friction that were noted at intervals during most tests [3]. After a short burst of two or three times the normal friction, the amount of wear debris between the seal ring surfaces decreased and friction coefficient returned to its steady value of about 0.09-0.10.

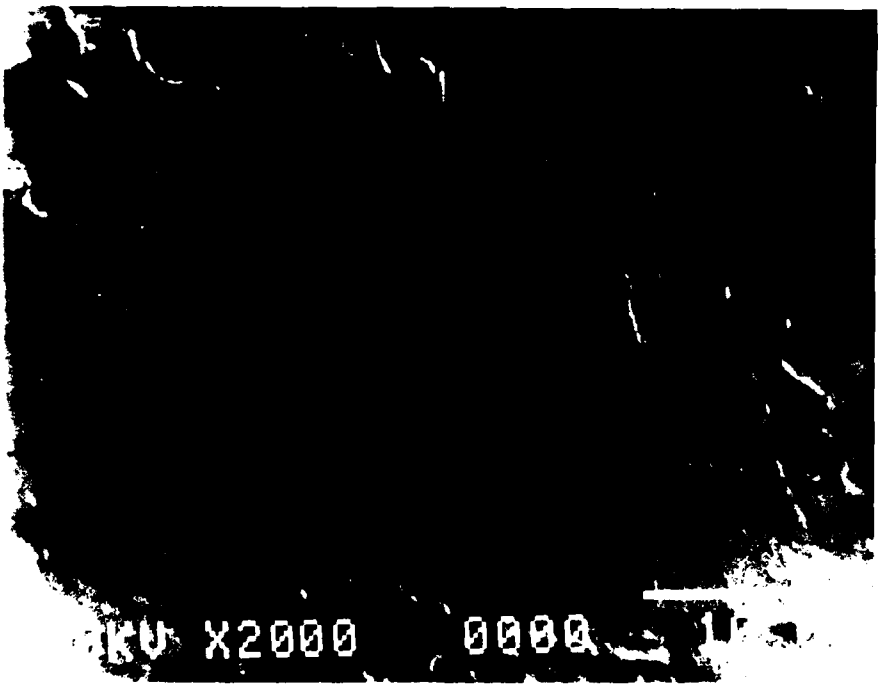

FIGURE 8. Worn surface of titanium nitride coating, showing carbon graphite transfer. (2000X magnification)

2.4.3 Chromium Carbide

Both of the chromium carbide coatings showed good wear resistance in these tests. On a volumetric basis their wear rates were, in fact, almost 50% lower than the wear rate of tungsten carbide, the next most wear resistant coating. On a mass loss basis the difference was even larger. Wear of the carbon graphite rings sliding against chromium carbide was no greater than against any of the other coatings. Coating H, which had the smaller nickel chromium particle size and slightly lower density, had slightly more wear resistance than coating C (on a mass loss basis), and also caused less carbon graphite wear. Coating H had also proven to have more erosion resistance than coating C in tests by Sue and Tucker [8].

Examination of the worn surfaces of both chromium carbide coatings showed that wear had been by a light polishing mechanism. An example is shown in Figure 9, which is an optical micrograph of a worn C coating. No significant differences in appearance were noted between the two chromium carbide coatings. Transferred carbon and loose carbon graphite debris were found on the worn coating surfaces, as can be seen in Figure 9. The wear grooves on the surface were shallow, indicating that there were no large abrasive third body particles in the interface. This indicates that there was little pullout of carbide particles. More evidence for that conclusion and for the conclusion that wear was by a polishing mode is presented in the surface profiles of Figure 10.

Figures 10A and 10B show profiles of the chromuim carbide coating before and after, respectively, a 6 hour (100 km) sliding test. It can be seen from the profiles that there was no increase in either number or depth of the grooves on the surface, but there was some wear of the asperity peaks. This resulted in a small decrease in surface roughness (from 0.068μm to 0.051μm Ra in this case). The wear of the peaks, most of which are chromium carbide particles, would result in the production of very fine wear debris, a conclusion that is consistent with observations of the worn surfaces.

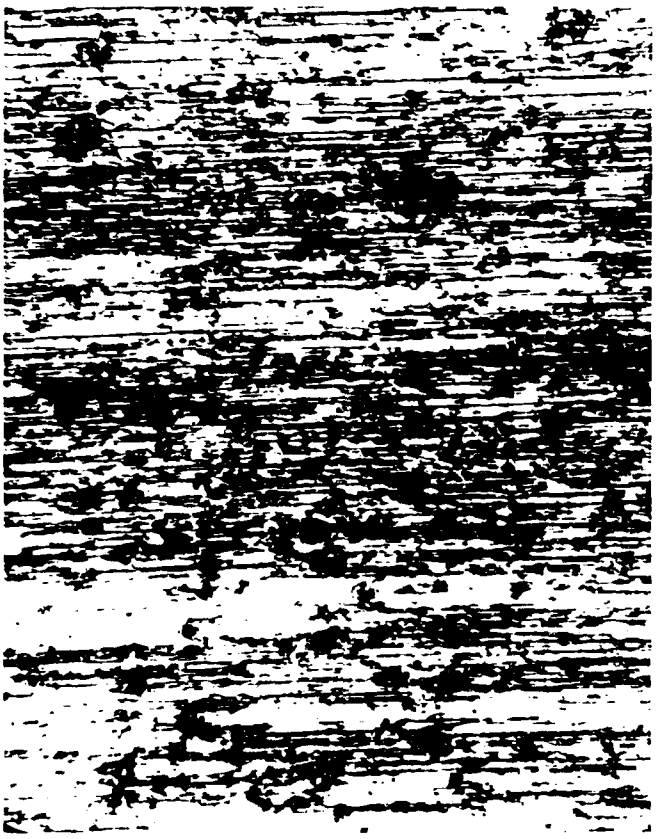

FIGURE 9. Optical micrograph of worn chromium carbide C coating. (200X)

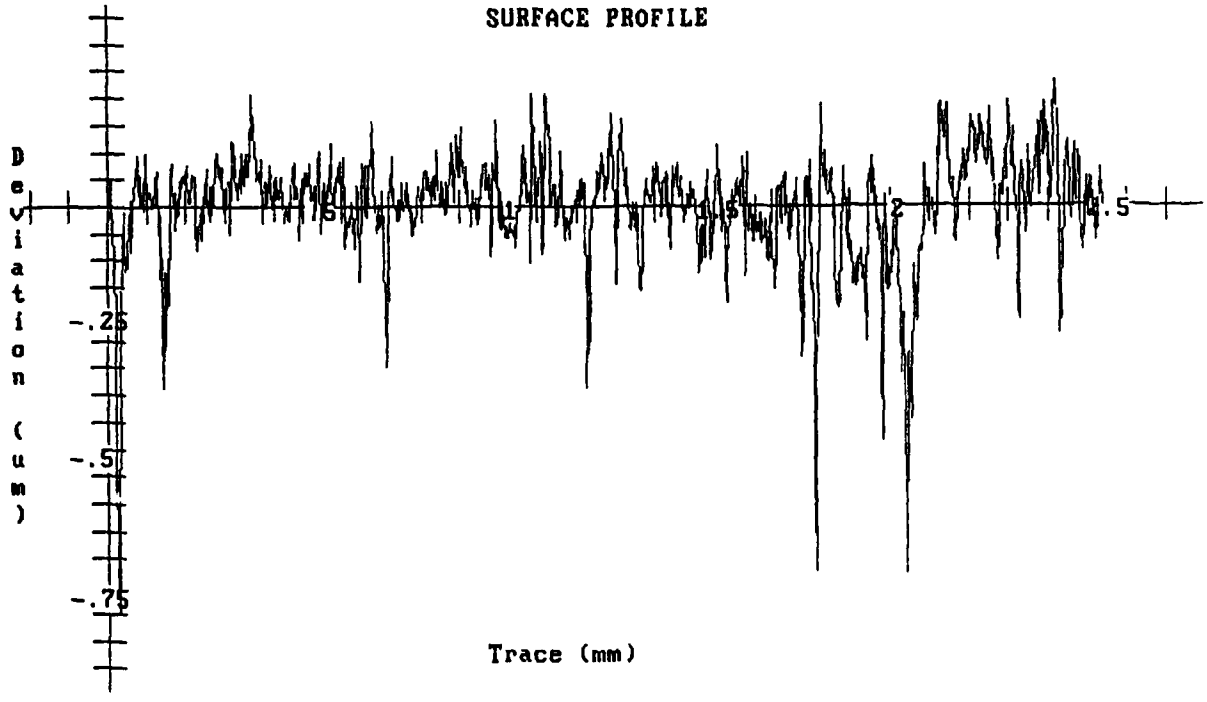

FIGURE 10A. Surface profile of chromium carbide C ring before 6 hour wear test.

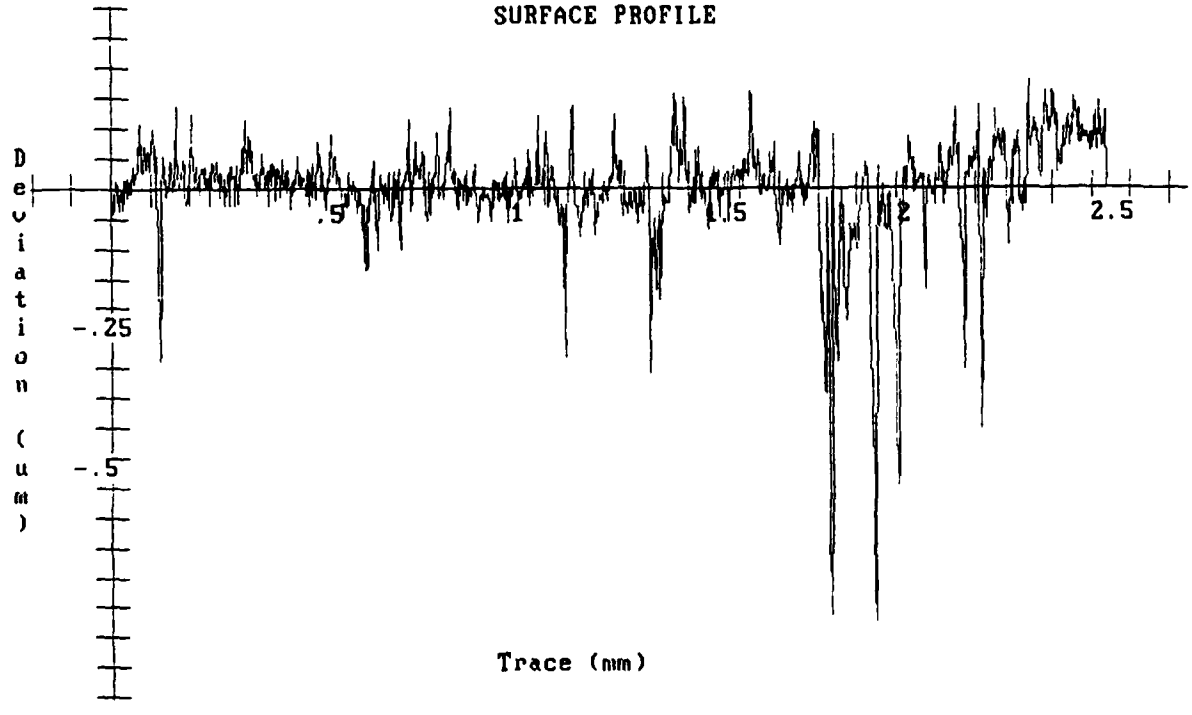

FIGURE 10B. Surface profile of chromium carbide C ring after 6 hour wear test.

2.4.4 Chromium Oxide

Plasma-sprayed Cr_2O_3 coatings also had very low wear rates, a bit lower than TiN but higher than chromium carbide. They also appeared to wear by a process of polishing of surface asperities, resulting in a slight (about 10%) decrease in surface roughness (Ra). There was little evidence of abrasion by the Cr_2O_3 coating. The friction coefficient was a bit higher than was measured with either TiN or WC, but was still only approximately 0.10. Despite the good wear behavior of Cr_2O_3, there was still a durability problem; in this case, thermocracking. Radial cracks were observed in the wear track on the coating surface, and one example is shown in Figure 11. A cross-section of a typical crack is shown in Figure 12. Since the cracks were wider at the top than near the substrate interface (Figure 12), they appeared to be surface originated. The deepest cracks were blunted at the coating/substrate interface. Similar thermocracks had been observed in seawater-lubricated seals by Tribe and Green [4]. The cracks could limit the durability of the surfaces because small chips of coating material could be liberated at the edges of the cracks. This could lead to more three-body abrasion by the debris and more abrasive wear of the carbon graphite surface by the crack edges, although there was little evidence of such damage in these tests at 100 N normal load. Several tests were also run at a higher load (750 N) and it was found that the number and size of thermocracks was considerably larger at the higher load. There was also some evidence of abrasion of the carbon graphite surface by debris from the cracks at the higher load.

A thermomechanical analysis was carried out to help explain the cause of the cracking (below).

2.5 Results of Corrosion Tests

One of the concerns about durability of ceramic-coated seal rings stems from their tendency to corrode at the coating/substrate interface, as had been noted by Tribe [2]. The substrate material, Inconel 625, was chosen for this study to limit the possibility of corrosion. To check the corrosion behavior of these coatings, samples of each coating were placed in an agitated bath of seawater for periods of 30 and 60 days. The specimens were weighed both before and after the tests and they were examined in optical and

FIGURE 11. Worn surface of chrome oxide coating, showing radial crack. (1000X magnification)

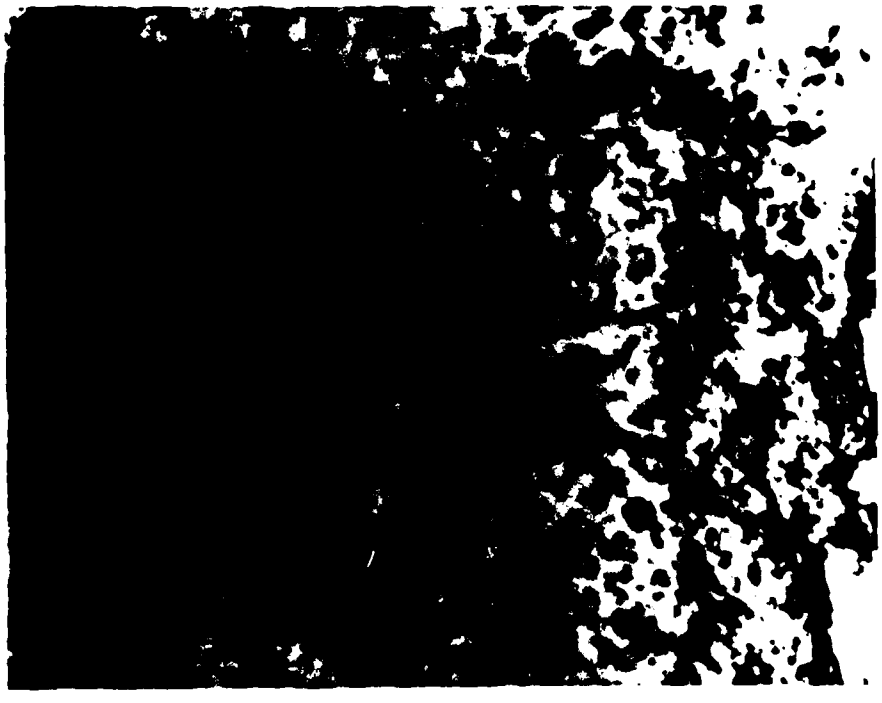

FIGURE 12. Cross-section of crack in chrome oxide coating. (500X magnification)

scanning electron microscopes after coming out of the salt water bath. There was no evidence of any corrosion for titanium nitride, chromium carbide or chromium oxide coatings. The weight of those specimens did not change measurably and microscopic observation showed no change in appearance resulting from the salt water environment.

The tungsten carbide specimens did show some evidence of corrosion and some buildup of salt deposits. These indications occurred in the interface region where diffusion had occurred between coating and substrate. An SEM micrograph of that region is shown in Figure 13. The section had been polished before being placed in the salt water solution for 30 days. The grain boundaries can be clearly seen in the micrograph, and it is evident that portions of the grain boundaries had resisted corrosive attack better than other material in and adjacent to the grain boundaries. This effect was noted only in the Inconel substrate near the interface with the coating. Evidently, during the heat treatment carbon diffused from the coating and combined with chromium at the grain boundaries to form chrome carbides. This depleted some of the corrosion-resisting chromium in portions of the grain boundaries and led to some corrosion. Although the corrosion was not severe in this case, and was not significantly different after 60 days in the solution, it did indicate that corrosion could become a problem with heat treated coatings. The diffusion processes that lead to a better coating/substrate bond could also result in a lessening of the corrosion resistance at the coating/substrate interface by sensitization of the Inconel 625 material. It should be noted that the subsurface region in which the corrosion was noted is not normally exposed to salt water in a seal application.

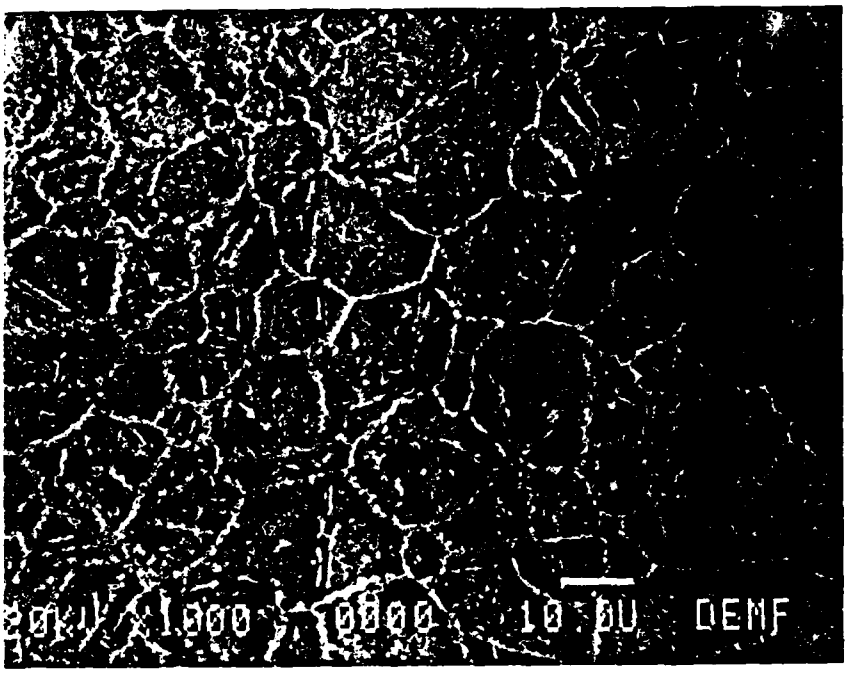

FIGURE 13. Cross-section of tungsten carbide - coated specimen after 30 days in salt water solution. Photograph shows region approximately 300 μm beneath worn surface, at interface between coating (right) and inconel substrate (left). (1000X magnification)

3.0 ANALYTICAL

3.1 Methods

In an attempt to understand the reasons for coating failure, especially the thermocracking noted with Cr_2O_3 coatings, an analytical study of thermal and thermo-mechanical phenomena near the sliding contacts was carried out. The analysis was done using finite element methods which are described in detail elsewhere [6]. The primary components of the analysis were a determination of the temperature distribution in the sliding contact region and an analysis of the stresses and deformations caused by the temperature distribution, along with mechanical normal and tangential tractions. The temperatures were calculated using a finite element thermal analysis program, Thermap, that was developed especially to analyze the effects of frictional heating of sliding contacts. Thermo-elastic and thermo-elastic-plastic stress analyses were done using the Adina finite element program. A suite of interconnected programs was developed to automatically generate the finite element mesh, generate the boundary condition files, run Thermap and Adina, and plot the output [6].

Boundary conditions for the finite element analysis were determined from the experiments described earlier. Measured values of friction force, along with the applied normal load and sliding velocity, were input to the analysis programs. The normal force was assumed to be uniformly distributed along the top surface of the Inconel 625 ring and the friction force was assumed to be applied through the thickness of that ring. The carbon graphite ring was assumed to be supported on a rigid support and to have its rotation restrained by rigid anti-rotation slots. Temperatures of the back faces of both seal rings were measured in the sliding tests and were prescribed on the finite element model. All boundary conditions are shown schematically in Figure 14.

The ring geometry used in the finite element model was similar to the geometry of the test seal rings. Earlier work [3] had shown that the rings are in actual solid/ solid contact only over a portion of their circumference. For this analysis it was assumed that contact occurred in five spots equidistantly spaced along the ring surface. It was assumed that all

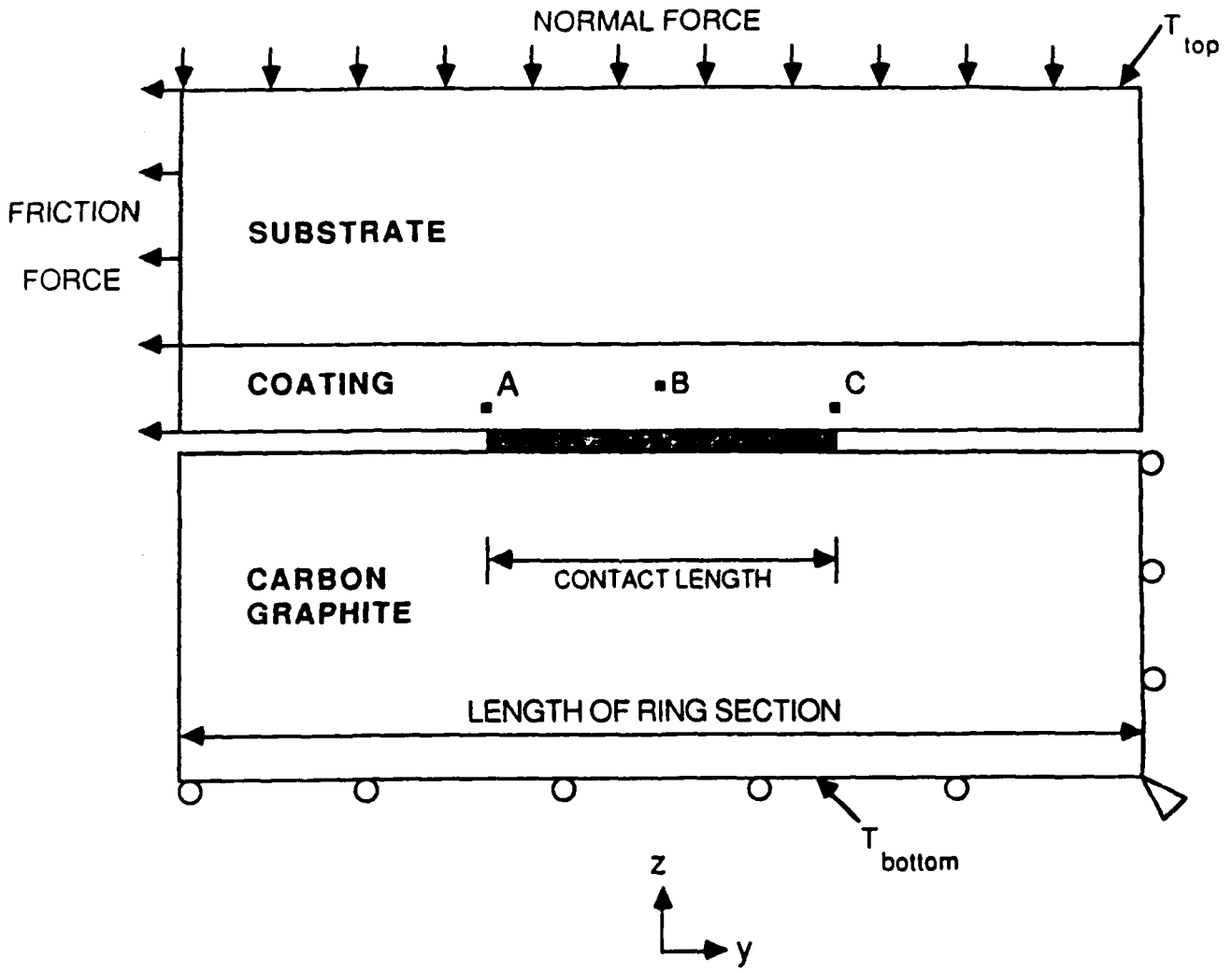

FIGURE 14. Diagram of region modelled in finite element analysis, showing boundary conditions applied.

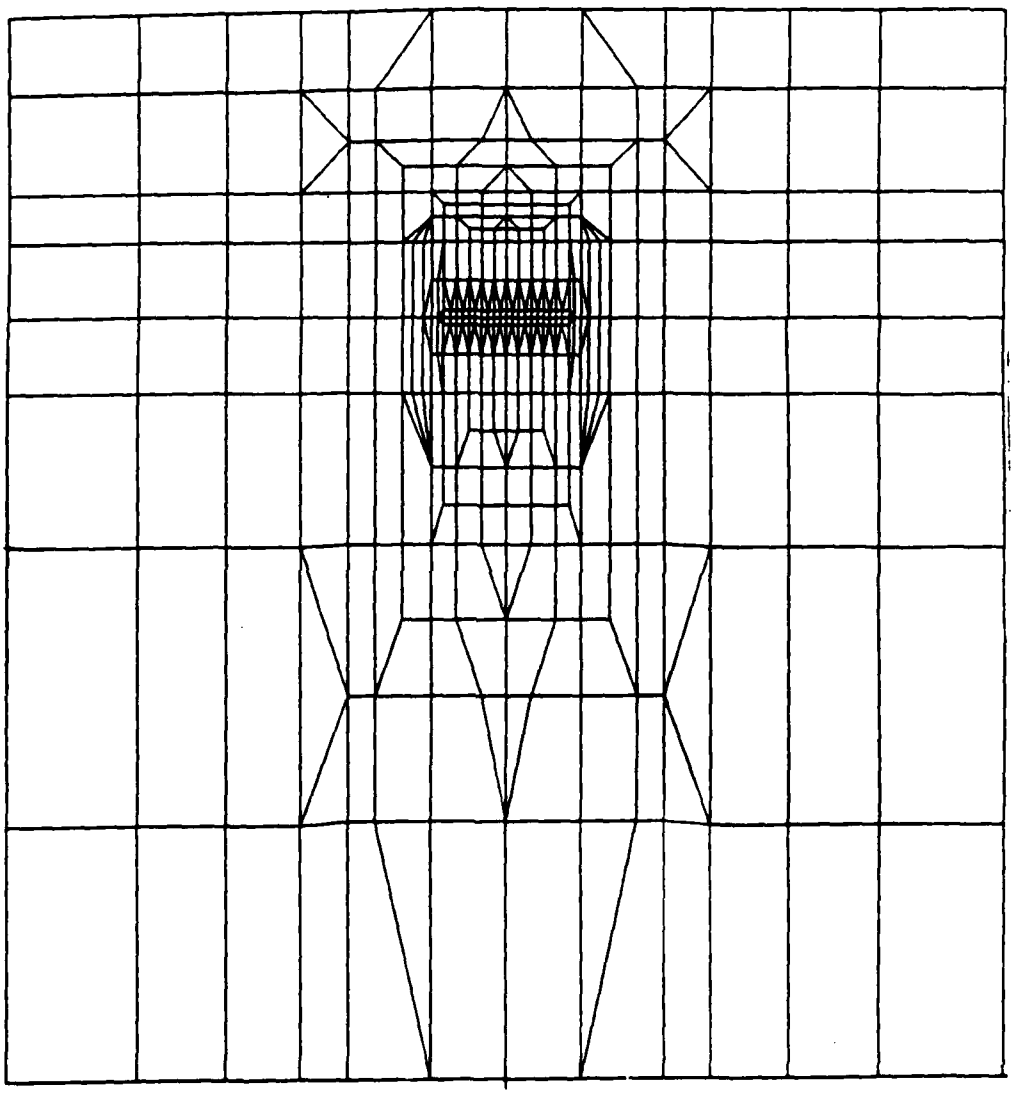

FIGURE 15. Typical finite element mesh used in analysis of ring section. Contact region contains smallest elements.

contact spots was identical and that a typical contact length was 1 mm. Only one such spot was analyzed, as is shown in Figure 14. These assumptions were based on measurements of contact sizes for WC-coated rings sliding against carbon graphite, with the measurements having been made using a unique contact probe [3].

A two dimensionsal finite element mesh was generated for the typical contact case and that mesh was stretched or shrunk to fit other contact lengths. The mesh had very small elements in the contact region to accurately model temperature and stress gradients there. Frictional heat was assumed to be uniformly distributed among the elements along the length of the contact. The rate of frictional heating was determined from measured friction force and velocity values. A typical finite element mesh is shown in Figure 15.

3.2 Results

Temperatures and stresses were analyzed for all of the coatings tested in the experimental program and for several different values of coating thickness and contact length. Isotherms from a Thermap analysis of sliding contact between a Cr_2O_3-coated ring and carbon graphite are shown in Figure 16. The maximum temperature in this and other material combinations occurred on the contact surface in the trailing portion of the contact zone. Temperature gradients were greatest in the contact region, particularly in the coating. Cr_2O_3, which has the lowest thermal conductivity of the four coatings studied, had the highest maximum surface temperature and the largest temperature gradients. For example, for a coating thickness of 250 μm, a contact length of 1 mm, and a normal load of 20 N per contact, the maximum surface temperature for the chrome oxide coating was 281°C, while for titanium nitride and tungsten carbide the maximum surface temperatures were 206 and 198°C, respectively.

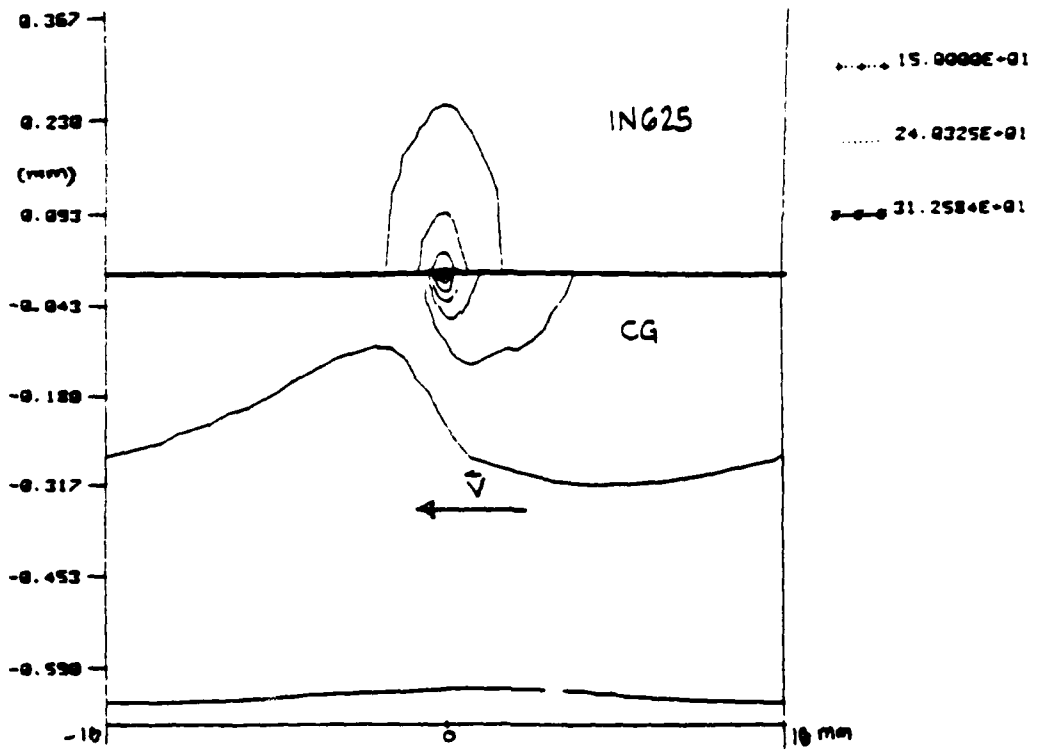

FIGURE 16. Typical isotherms predicted for case of chromium oxide coating on Inconel 625 (top) sliding against carbon graphite ring (bottom)

Surface temperature predictions for some of the Cr_2O_3 coatings studied are shown in Table 3. It can be seen that contact length had a significant influence on maximum surface temperature, owing to the fact that frictional heat flux increased with a decrease in contact length. The influence of coating thickness was a bit less significant. Although an increase in thickness of the chrome oxide coating led to an increase in temperature, that effect was not noted with coatings with higher thermal conductivity, such as tungsten carbide. For those coatings an increase in coating thickness led to a slight decrease in surface temperature. An even more important factor proved to be load per contact. If the normal load increased, or the number of contact spots decreased, the frictional heat flux would increase, resulting in higher surface temperatures.

TABLE 3

TEMPERATURE AND STRESS IN CHROME OXIDE COATED RING

Effect of various operating and geometric parameters on maximum surface temperature and maximum tensile stress in coating and maximum effective (von Mises) stress in Inconel 625 substrate. Thermoelastic analysis.

Coating thickness (mm)	0.075	0.25	0.25	0.35	0.35
Contact length (mm)	1.0	1.0	0.25	1.0	1.0
Normal load per contact spot (N)	20	20	20	20	150
Maximum surface temperature (°C)	258	281	386	313	926
Maximum principal stress in coating (Mpa)	65	40	142	63	779
Maximum effective stress in substrate (MPa)	446	395	394	484	1075

Stresses in the contact region included contributions from both mechanical tractions and temperature gradients. In the cases studied, where the sliding velocity was high enough to cause significant frictional heat generation and temperature gradients, the thermal contribution proved to be dominant. This is in agreement with the conclusions of Ju and Chen [8]. The result of this was a state of stress that was predominantly tensile in the coating and compressive in the adjacent substrate. As had been found earlier by Ju and Chen [8] for other coating/substrate combinations, the largest computed tensile stress in the coating occurred at the contact surface near the trailing edge of the contact (point C in Figure 14). The magnitude of that tensile stress was significantly affected by both the length of a contact spot and and the normal load per contact spot, as can be seen in Table 3.

We can conclude, therefore, that the factors that most affect the frictional heat generation rate and surface temperature also have a great effect on tensile stress in the coating. That tensile stress could become large enough to cause a crack to form and propagate in the coating. The largest tensile stress component was found to act in the circumferential direction and occurred at or near the contact surface. Thus it is to be expected that any cracks resulting from that state of stress would be radial and would be surface originated. This is in agreement with the crack orientation observed in the experimental work described above. In addition to causing significant tensile stress in the coating, the temperature gradients also caused substantial compressive stress in the adjacent substrate. The substrate stresses could be large enough to result in plastic deformation if the substrate material was soft enough.

The stress calculations in Table 3 were all done for the thermoelastic case, that is it was assumed that no yielding occurred in any of the materials. Some thermo-elasto-plastic analyses were also done. It was found that if the substrate deformed plastically (in compression), the coating above it would see even larger tensile stress. For example, for the case listed in the last column of Table 3, if the substrate had a yield strength of 490 MPa, the maximum tensile stress in the coating would increase to 864 MPa (from 779

MPa) due to plastic deformation in the substrate. This result is shown, along with computed temperatures and stresses for many other cases, in Table 4. Therefore, a coated system with a softer substrate would be expected to experience even more thermocracking of the coating than if the substrate was harder.

TABLE 4

COMPUTED TEMPERATURES AND STRESSES FOR VARIOUS COATING MATERIALS AND THICKNESSES

Materials: CR = Chromium Oxide, TN = Titanium Nitride, NWC = Tungsten Carbide, IN625 = Inconel 625, CG = carbon graphite

hl indicates high load (150N/ per contact spot), hlp indicates lower yield strength (490 MPA for substrate). All other runs assumed 20N/spot and 1100MPa substrate yield strength.

Run / Parameter	CR 3275	CR 3225	CR 3235	CR 32250	CR 2525	CR 425	CR 2535	CR hl	CR hlp	TN 3275	TN 3225	NWC 3275	NWC 3225
Contact mesh width (mm)	1.0	1.0	1.0	1.0	0.25	4.0	0.25	1.0	1.0	1.0	1.0	1.0	1.0
Coating thickness (mm)	0.075	0.25	0.35	0.25	0.25	0.25	0.35	0.35	0.35	0.075	0.25	0.075	0.25
Bottom ring temp. (^{o}C)	100	100	150	150	100	100	100	150	150	100	100	100	100
Von Mises IN625 (MPa)	446	395	484	497	394	356	371	1075	490	419	373	432	377
Von Mises Coat. (MPa)	192	194	224	225	264	190	261	889	925	461	390	445	375
Von Mises CG (MPa)	64	60	76	74	119	73	121	516	520	60	50	63	53
Maximum temp. (^{o}C)	258	281	313	310	386	192	387	926	926	213	206	214	198
Heat production (W)	6.7	6.7	6.7	6.7	6.7	6.7	6.7	32	32	5.7	5.7	6.2	6.2
Coating Stress (MPa) t=2	141	141	174	174	142	72	144	779	864	412	362	397	353

4.0 CONCLUSIONS

Each of the coatings tested in this program, tungsten carbide, titanium nitride, chromium carbide and chrome oxide, all on Inconel 625 substrates, had low wear rates and low friction during sliding against carbon graphite seal rings. The wear rates were lower than for metallic seal face materials and nearly as low as had been determined for monolithic silicon carbide. Despite the good friction and wear results, most of the coatings displayed a deficiency which could limit its durability in salt water sealing applications.

Owing to the slow nature of the PVD coating process, titanium nitride coatings have a limited thickness. Although they have low wear rates when the coating is intact, the wear is finite and eventually the coatings get quite thin. When this happens there is a tendency for the coatings to spall and this results in a very significant increase in wear rate, owing to the presence of hard, abrasive third bodies between the seal faces.

Tungsten carbide coatings show evidence of some surface pitting resulting from both initial porosity and the occasional spalling of a carbide particle from the surface. The amount of pitting can be reduced and the bond strength of the coating/substrate interface can be increased by heat treating the coated rings. Diffusion processes during the heat treatment can reduce the resistance of the Inconel 625 substrate to corrosion in salt water by sensitizing the material at the grain boundaries in the region adjacent to the coating.

Although chrome oxide coatings have good wear resistance, they show a tendency to thermocrack. The cracks originate on the sliding surface and are oriented perpendicular to the sliding direction. The severity of thermocracks increases with increases in normal load.

Thermal and stress analyses of the contact region of coated rings showed that frictional heating causes surface temperature increases which can result in tensile stress in the coatings. The surface temperatures and resulting tensile thermal stress are higher if the coating has a low thermal conductivity, as is the case with chrome oxide. The highest tensile stress acts in the sliding direction and occurs at the sliding surface. Thus, that stress is probably responsible for the thermocracking observed with chrome oxide

coatings in this test program. The tensile stress is increased if the substrate deforms plastically. Thus it is expected that more coating thermocracking would result with softer substrates.

The chromium carbide coatings displayed the lowest wear rates of all the coatings tested. Wear of the carbon graphite in contact with the chromium carbide rings was also less than or equal to that measured with the other coatings. The chromium carbide coating with the smaller nickel chromium particle size (coating H) showed even better wear resistance than did the other chromium carbide coating tested. Neither of the chromium carbide coatings showed any evidence of thermocracking in the tribotests, nor did they show evidence of corrosion after immersion in salt water. For these reasons, chromium carbide coatings appear to be good candidates for potential saltwater face seal applications. It is recommended that the performance of those coating materials be further studied in actual face seals.

5.0 REFERENCES

1. White, E.B. and Karpe, S.A., "Evaluation of Mechanical Face Seal Materials", Lubrication Engineering, v. 41 (1985), 675-680

2. Tribe, F.J., "Seawater-Lubricated Mechanical Seals and Bearings: Associated Materials Problems", Lubrication Engineering, v. 39 (1983), 292-299

3. Kennedy, F.E., Hussaini, S.Z. and Espinoza, B.M., "Contact Conditions and Wear of Hard Seal Faces Against Carbon Graphite", Lubrication Engineering, v. 44 (1988), 361-367

4. Tribe, F.J. and Green, G.A., "Assessment of Mechanical Seal Face Materials Under Controlled Interface Torque", Lubrication Engineering, v. 42 (1986), 686-693

5. Ramalingam, S., "New Coating Technologies for Tribological Applications", in M.B. Peterson, ed., Wear Control Handbook, ASME, New York (1981), 385-411

6. Kennedy, F.E., Grim, J.N. and Chuah, C.K., "An Experimental/Theoretical Study of Contact Phenomena in Mechanical Face Seals", in Developments in Numerical and Experimental Methods Applied to Tribology, Butterworths, London (1984), 138-150.

7. Kennedy, F.E. and Hussaini, S.Z., "Thermomechanical Analysis of Dry Sliding Systems", Computers and Structures, v. 26 (1987), 345-355.

8. Sue, J.A. and Tucker, R.C., "High Temperature Erosion Behavior Tungsten- and Chromium-Carbide-Based Coatings", Surface and Coatings Technology, v.32 (1987), 237-248.

9. Ju, F.D. and Chen, T.Y., "Thermomechanical Cracking in Layered Media from Moving Friction Load", ASME Journal of Tribology, v. 106 (1984), 513-518.

END

DATE

FILMED

DTIC

9-88